PRAMANA
— journal of
physics

© Indian Academy of Sciences

Vol. 72, No. 1
January 2009
pp. 55–68

Transverse spin and momentum correlations in quantum chromodynamics

LEONARD P GAMBERG
Department of Physics, Penn State University-Berks, Reading, PA 19610, USA
E-mail: lpg10@psu.edu

Abstract. The naive time reversal odd ('T-odd') parton distribution and fragmentation functions are explored. We use the spectator model framework to study flavour dependence of the Boer–Mulders ($h_1^\perp$) and Sivers ($f_{1\mathrm{T}}^\perp$) functions as well as the 'T-even' but chiral odd function $h_{1\mathrm{L}}^\perp$. These transverse momentum-dependent parton distribution functions are of significance for the analysis of azimuthal asymmetries in semi-inclusive deep inelastic scattering, as well as for the overall physical understanding of the distribution of transversely polarized quarks in unpolarized hadrons. In this context we also consider the Collins mechanism and the fragmentation function $H_1^\perp$. As a by-product of this analysis we calculate the leading twist unpolarized $\cos(2\phi)$ asymmetry, and $\sin(2\phi)$ single spin asymmetry for a longitudinally polarized target in semi-inclusive deep inelastic scattering.

Keywords. Partons; intrinsic transverse momentum; transversity.

PACS Nos 13.85.Ni; 12.38.Cy; 12.39.St

1. Introduction

Transverse momentum-dependent (TMD) parton distributions (PDFs) have gained considerable attention in recent years. Theoretically they can account for non-trivial transverse spin and momentum correlations such as single spin asymmetries (SSAs) in hard scattering processes when transverse momentum scales are on the order of quarks in hadrons, namely, $P_{\mathrm{T}} \sim k_\perp \ll \sqrt{Q^2}$. For example, the Sivers function $f_{1\mathrm{T}}^\perp$ [1] which accounts for the observed SSA in semi-inclusive deep inelastic scattering (SIDIS) for a transversely polarized proton target by the HERMES Collaboration [2] describes correlations of the intrinsic quark transverse momentum and the transverse nucleon spin. The corresponding SSA on a deuteron target measured by COMPASS [3] vanishes, indicating a flavour dependence of the Sivers function. Another leading twist 'T-odd' PDF, the chiral-odd Boer–Mulders function $h_1^\perp$ [4] describes correlations between the transverse spin of a quark and its transverse momentum within the nucleon. Theoretically, twist two 'T-odd' PDFs are of particular interest as they emerge from the colour gauge invariant definition of the quark-gluon-quark correlation function [5–7]. The gauge link not only ensures a colour gauge invariant definition of correlation functions, but it also describes

initial/final (ISI/FSI) state interactions [8–10] which can generate SSAs [8,11,12]. Assuming factorization of leading twist SIDIS spin observables in terms of the 'T-even'and 'T-odd' TMD PDFs and fragmentation functions (FFs) [13], refs [4,14] show how spin observables in SIDIS can be expressed in terms of convolutions of these functions.

Here I report on work with Goldstein and Schlegel [15], where we explore the flavour dependence of the twist-2 'T-odd' Boer–Mulders function $h_1^\perp$ and Sivers $f_{1\mathrm{T}}^\perp$ TMD PDFs as well as work with Bacchetta, Goldstein and Mukherjee [16], where we calculate Collins fragmentation function $H_1^\perp$ [17]. The Boer–Mulders and Collins functions are particularly important for the analysis of the azimuthal $\cos(2\phi)$ asymmetry in unpolarized SIDIS. We employ the factorized approach used in refs [12,18]. In the partonic picture, the Boer–Mulders function is convoluted with the 'T-odd' (and chiral-odd) Collins fragmentation function $H_1^\perp$. Although these azimuthal asymmetries were measured in SIDIS by the ZEUS Collaboration [19,20] and in Drell–Yan (DY) [21,22], little is known about the Boer–Mulders function. Of particular interest is the sign for different flavours u and d since this significantly affects predictions for these asymmetries. We also consider the flavour dependence of the 'T-even' function $h_{1\mathrm{L}}^\perp$, which is of interest in the transverse momentum and quark spin correlations in a longitudinally polarized target [23].

2. TMD correlators in the spectator framework

Transverse momentum quark distribution and fragmentation functions contain essential non-perturbative information about the partonic structure of hadrons. In principle their moments are calculable from first principles in lattice QCD. A great deal of understanding has also been gained from model calculations using the spectator framework. In addition to exploring the kinematics and pole structure of the TMDs [24–27], phenomenological estimates for 'T-even' PDFs [18] (see also [28]) and FFs [29] and for 'T-odd' PDFs [9–12,15,30–33] have been carried out.

We start (see [18]) from the definition of the unintegrated, colour gauge invariant, quark–quark correlator

$$\Phi_{ij}(x,\vec{p}_{\mathrm{T}}^{\,2}) = \sum_X \int \frac{\mathrm{d}\xi^- d^2\xi_{\mathrm{T}}}{(2\pi)^3} \times \mathrm{e}^{ip\cdot\xi}\langle P,S|\bar{\psi}_j(0)\mathcal{U}^n_{(0,\infty)}|X\rangle\langle X|\mathcal{U}^n_{(\infty,\xi)}\psi_i(\xi)|P,S\rangle|_{\xi^+=0}, \quad (1)$$

where the gauge link $\mathcal{U}^C_{(\zeta,\xi)} = \mathcal{P}\exp\{-ig\int_\zeta^\xi \mathrm{d}\eta\cdot A(\eta)\}$ and C designates the process-dependent (see [34]) integration path with endpoints ζ and ξ. In an arbitrary gauge there is a contribution at light cone infinity pointing in transverse directions [6,7]. We work in Feynman gauge where the transverse Wilson line vanishes [6]. In the spectator model the sum over a complete set of intermediate on-shell states $|X\rangle$ is represented by a single one-particle diquark state $|dq;p_{dq},\lambda\rangle$, where p_{dq} is the diquark momentum and λ its polarization. Since the diquark is 'built' from two valence quarks it can be a spin 0 (scalar diquark) or a spin 1 (axial-vector diquark) particle. By applying a translation on the second matrix element in eq. (1) we can

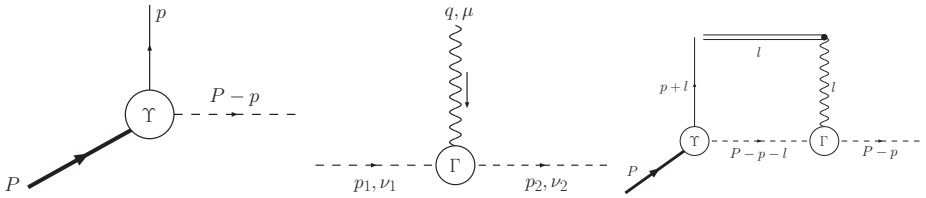


Figure 1. Vertices for the proton–quark–diquark, gluon–diquark, and contribution of the gauge link in the one-gluon approximation.

integrate out ξ and perform the momentum integration over the diquark momentum p_{dq} to obtain the form of the correlator,

$$\Phi_{ij}(p;P,S) = \sum_{\lambda} \frac{\delta((P_s)^2 - m_s^2)\Theta(P_s^0)}{(2\pi)^3} \langle P,S|\,\bar{\psi}_j(0)\mathcal{U}^n_{(0,\infty)}|\,dq;\,P_s,\lambda\rangle \times\langle\, dq;\,P_s,\lambda|\,\mathcal{U}^n_{(\infty,\xi)}\,\psi_i(0)\,|P,S\rangle. \tag{2}$$

2.1 *Naive time reversal-even ('T-even') PDFs*

The essence of the diquark spectator model for TMD PDFs is to calculate the matrix elements in eq. (2) by the introduction of effective nucleon–diquark–quark vertices $\Upsilon_s(N)$ (scalar) and $\Upsilon^{\mu}_{\rm ax}(N)$ (axial-vector), which are represented in the left panel of figure 1. For example, the matrix element for the axial vector diquark is

$$\langle adq;\,P_s;\lambda|\,\psi_i(0)\,|P,S\rangle = i\frac{g_{\rm ax}(p^2)}{\sqrt{3}}\varepsilon^*_{\mu}(P_s;\lambda) \times\frac{\left[(\not{p}+m_q)\gamma_5\left[\gamma^{\mu} - R_g\frac{P^{\mu}}{M}\right]u(P,S)\right]_i}{p^2 - m_q^2 + i0}, \tag{3}$$

where the polarization vector of the axial-vector diquark is ε_{μ} and $u(P,S)$ denotes the nucleon spinor where M and m_q are nucleon and quark masses respectively. We consider the diquark as an on-shell particle with mass m_s, momentum $P_s = P - p$ where the polarization sum for the axial-vector diquark is

$$\sum_{\lambda}\varepsilon^*_{\mu}(P_s;\lambda)\varepsilon_{\nu}(P_s;\lambda) = -g_{\mu\nu} + \frac{(P_s)_{\mu}(P_s)_{\nu}}{m_s^2}. \tag{4}$$

The unpolarized TMD f_1 is obtained by inserting these expressions into eq. (2) and projecting from the quark–quark correlator

$$f_1(x,\vec{p}_{\rm T}^{\,2}) = \frac{1}{4}\int {\rm d}p^-\left({\rm Tr}\left[\gamma^+\Phi\left(p;P,S\right)\right] + {\rm Tr}\left[\gamma^+\Phi\left(p;P,-S\right)\right]\right)\Big|_{p^+=xP^+}, \tag{5}$$

where the '+' sign of the γ-matrix denotes the usual light cone component ($a^{\pm} = 1/\sqrt{2}(a^0 \pm a^3)$). The results for f_1 in the scalar and axial-vector diquark sectors are

$$f_1^{\rm sc}(x,\vec{p}_{\rm T}^{\,2}) = \frac{|g_{\rm sc}(p^2)|^2}{2(2\pi)^3}\frac{(1-x)[\vec{p}_{\rm T}^{\,2}+(xM+m_q)^2]}{[\vec{p}_T^{\,2}+\tilde{m}^2]^2},$$
$$f_1^{\rm ax}(x,\vec{p}_{\rm T}^{\,2}) = \frac{|g_{\rm ax}(p^2)|^2}{6(2\pi)^3}\frac{\mathcal{R}_1^{\rm ax}\left(x,\vec{p}_{\rm T}^{\,2};R_g,\{\mathcal{M}\}\right)}{M^2 m_s^2(1-x)[\vec{p}_{\rm T}^{\,2}+\tilde{m}^2]^2}, \tag{6}$$

where $\tilde{m}^2 \equiv xm_s^2 - x(1-x)M^2 + (1-x)m_q^2$. To shorten the somewhat lengthy expression for the axial-vector contribution we introduce a function $\mathcal{R}_1^{\rm ax}$ depending on x and $\vec{p}_{\rm T}$, the model parameter R_g, and the set of masses $\{\mathcal{M}\} \equiv \{M, m_s, m_q\}$ which is given in Appendix C of ref. [15]. Another 'T-even' but chiral-odd function of interest is the distribution of transversely polarized quarks in a longitudinally polarized target,

$$\frac{4\lambda_{\rm P} p_{\rm T}^i}{M} h_{1\rm L}^{\perp}(x,\vec{p}_T^{\,4}) = \int {\rm d}p^- \{{\rm Tr}[\gamma^+\gamma^i\gamma_5\Phi(p;P,S_{\rm L})] - {\rm Tr}[\gamma^+\gamma^i\gamma_5\Phi(p;P,-S_{\rm L})]\}, \tag{7}$$

where $\lambda_{\rm P}$ is the target helicity and $S_{\rm L}$ is the spin 4-vector in longitudinal direction, i.e. $S_{\rm L} = (-\frac{\lambda_{\rm P}}{M}P^-, \frac{\lambda_{\rm P}}{M}P^+, \vec{0}_{\rm T})$. By applying similar methods as for f_1, we obtain

$$h_{1\rm L}^{\perp,{\rm sc}}(x,\vec{p}_{\rm T}^{\,2}) = -\frac{|g_{\rm sc}(p^2)|^2}{(2\pi)^3}\frac{(1-x)M(xM+m_q)}{\left[\vec{p}_T^{\,2}+\tilde{m}^2\right]^2},$$
$$h_{1\rm L}^{\perp,{\rm ax}}(x,\vec{p}_{\rm T}^{\,2}) = \frac{|g_{\rm ax}(p^2)|^2}{12(2\pi)^3}\frac{\mathcal{R}_{1\rm L}^{\perp,{\rm ax}}\left(x,\vec{p}_{\rm T}^{\,2};R_g,\{\mathcal{M}\}\right)}{[\vec{p}_{\rm T}^{\,2}+\tilde{m}^2]^2 M m_s^2(1-x)}, \tag{8}$$

where again for brevity $\mathcal{R}_1^{\rm ax}$ and $\mathcal{R}_{1\rm L}^{\perp,{\rm ax}}$ are given in Appendix C of [15].

2.2 *The 'T-odd' PDFs*

By contrast, 'T-odd' PDFs cannot be generated by simply considering the tree-level diagram (left panel of figure 1). In the spectator framework, the 'T-odd' PDFs [8] are generated by the gauge link in eq. (1) [9–12]. The so-called leading contribution can be obtained by expanding the exponential of the gauge link up to first order in the quark gluon coupling. This contribution results in a box diagram as shown in the right panel of figure 1 which contains an imaginary part/phase which is necessary for the existence of the 'T-odds'. We restrict ourselves to the case where one gluon models the FSIs. The contribution from the gauge link in the box diagram in figure 1 is given by the double line and the eikonal vertex $\frac{i}{[l\cdot v+i0]} \times (-ie_q v^\lambda)$, where l is the loop momentum, e_q the charge of the quark and $n = v$ is a light cone vector representing the direction of the Wilson line. In the box diagram we specify the gluon–diquark interaction for a scalar and axial-vector diquark with a general axial-vector–vector coupling that models the composite nature of the diquark through

an anomalous magnetic moment κ [35]. In the notation of figure 1 (centre panel) the gluon–diquark vertices are

$$\begin{aligned}\Gamma_s^{\mu} &= -ie_{dq}(p_1+p_2)^{\mu},\\ \Gamma_{\rm ax}^{\mu\nu_1\nu_2} &= -ie_{dq}[g^{\nu_1\nu_2}(p_1+p_2)^{\mu}\\ &\quad +(1+\kappa)(g^{\mu\nu_2}(p_2+q)^{\nu_1}+g^{\mu\nu_1}(p_1-q)^{\nu_2})].\end{aligned} \tag{9}$$

For $\kappa=-2$ the vertex $\Gamma_{\rm ax}$ reduces to the standard γWW-vertex. The matrix elements including the gauge link in the one gluon approximation are

$$\begin{aligned}\langle sdq;P_s|\mathcal{U}^{n-}_{(\infty,0)}\psi_i(0)\,|P,S\rangle|_{1-\rm gl} &= -ie_qe_{dq}\int\frac{{\rm d}^4l}{(2\pi)^4}g_{\rm sc}((l+p)^2)\\ &\times\mathcal{D}^{\rm sc}(P_s-l)\frac{[(\not p+\not l+m_q)u(P,S)]_i v\cdot(2P_s-l)}{[l\cdot v+i0][l^2+i0][(l+p)^2-m_q^2+i0]},\\ \langle adq;P_s,\lambda|\mathcal{U}^{n-}_{(\infty,0)}\psi_i(0)\,|P,S\rangle|_{1-\rm gl} &= -ie_qe_{dq}\int\frac{{\rm d}^4l}{(2\pi)^4}\,\frac{g_{\rm ax}((p+l)^2)}{\sqrt{3}}\varepsilon^*_{\sigma}(P_s,\lambda)\\ &\times\mathcal{D}^{\rm ax}_{\rho\eta}(P_s-l)\frac{[g^{\sigma\rho}\,v\cdot(2P_s-l)+(1+\kappa)(v^{\sigma}\,(P_s+l)^{\rho}+v^{\rho}\,(P_s-2l)^{\sigma})]}{[l\cdot v+i0][l^2+i0][(l+p)^2-m_q^2+i0]}\\ &\times\left[(\not p+\not l+m_q)\,\gamma_5\left(\gamma^{\eta}-R_g\frac{P^{\eta}}{M}\right)u(P,S)\right]_i,\end{aligned} \tag{10}$$

where the subscript, '1−gl' denotes one gluon exchange. In these expressions $\mathcal{D}(P)$ denotes the propagator of the scalar and axial-vector diquark. We obtain the Boer–Mulders function $h_1^{\perp}$ by inserting eq. (10) (and the tree-level scalar and axial-vector matrix elements (3)) into eq. (2) and projecting the following Dirac structure from quark–quark correlator

$$\begin{aligned}\frac{4\epsilon_{\rm T}^{ij}p_{\rm T}^j}{M}h_1^{\perp}(x,\vec p_{\rm T}^{\,2}) &= \int{\rm d}p^-({\rm Tr}[\Phi_{\rm unpol}(p,S)i\sigma^{i+}\gamma_5]\\ &\quad +{\rm Tr}[\Phi_{\rm unpol}(p,-S)i\sigma^{i+}\gamma_5])\Big|_{p^+=xP^+},\end{aligned} \tag{11}$$

where $\epsilon_{\rm T}^{ij}\equiv\epsilon^{-+ij}$ and $\epsilon^{0123}=+1$. For the purpose of describing the loop integration, we give the somewhat lengthy expression

$$\begin{aligned}&\epsilon_{\rm T}^{ij}p_{\rm T}^j h_1^{\perp,{\rm ax}}(x,\vec p_T^{\,2}) = \frac{-e_qe_{dq}}{8(2\pi)^3}\frac{M}{P^+(\vec p_{\rm T}^{\,2}+\tilde m^2)}\\ &\times\int\frac{{\rm d}^4l}{(2\pi)^4}\Bigg\{\frac{g_{\rm ax}((l+p)^2)g^*_{\rm ax}(p^2)\mathcal{D}_{\rho\eta}(P_s-l)}{3}\\ &\times\frac{\sum_{\lambda}\varepsilon^*_{\sigma}(P_s;\lambda)\varepsilon_{\mu}(P_s;\lambda)[g^{\sigma\rho}\,v\cdot(2P_s-l)+(1+\kappa)(v^{\sigma}\,(P_s+l)^{\rho}+v^{\rho}\,(P_s-2l)^{\sigma})]}{[l\cdot v+i0][l^2-\lambda^2+i0][(l+p)^2-m_q^2+i0]}\\ &\times{\rm Tr}\Big[(\not P+M)(\gamma^{\mu}-R_g\frac{P^{\mu}}{M})(\not p-m_q)\gamma^+\gamma^i(\not l+\not p+m_q)\\ &\times\Big(\gamma^{\eta}+R_g\frac{P^{\eta}}{M}\Big)\gamma_5\Big]\Bigg\}+{\rm h.c.}\end{aligned} \tag{12}$$

Since the numerator in eq. (12) contains at most the fourth power of the loop integral it can be written as $\sum_{i=1}^{4} N^{(i)}_{\alpha_1\ldots\alpha_i} l^{\alpha_1}\ldots l^{\alpha_i} + N^{(0)}$. The coefficients (tensors) $N^{(i)}_{\alpha_1\ldots\alpha_i}$ depend only on external momenta and can be computed straightforwardly. The integration over the light cone component l^+ results in an integral that is potentially ill-defined. This happens when $g(p^2)$ is a holomorphic function in p^2 and at least one of the Minkowski indices is light-like in the minus direction, e.g. $\alpha_1 = -$, $\alpha_2, \ldots, \alpha_i \in \{+, \perp\}$ resulting in an integral of the form $\int \mathrm{d}l^+ \, \delta(l^+)\Theta(-l^+)$, implying that $l^+ = 0$ and $l^- = \infty$. This signals a light cone divergence (see ref. [32]). One can handle such divergences by introducing phenomenological form factors with additional poles [15]

$$g_{\rm ax}(p^2) = \frac{(p^2 - m_q^2) f(p^2)}{\left[p^2 - \Lambda^2 + i0\right]^n}. \tag{13}$$

For $n \geq 3$, there are enough powers of l^+ to eliminate this divergence. $f(p^2)$ is a covariant Gaussian [15] which cuts off the $p_{\rm T}$ integrations and Λ is an arbitrary mass scale fixed by fitting f_1 to data (see below and [15] for details). The resulting Boer–Mulders function for an axial-vector diquark is then given by

$$h_1^{\perp,{\rm ax}}(x, \vec{p}_{\rm T}^{\,2}) = \frac{-e_q e_{dq} N_{\rm ax}^4}{48(2\pi)^4} \times \frac{(1-x)^3 \mathrm{e}^{-\tilde{b}\vec{p}_{\rm T}^{\,2} - 2\tilde{b}(x m_s^2 - x(1-x)M^2)} \mathcal{R}_1^{\perp,{\rm ax}}\left(x, \vec{p}_{\rm T}^{\,2}; R_g, \kappa, \tilde{b}, \Lambda, \{\mathcal{M}\}\right)}{m_s^4 \left[\vec{p}_{\rm T}^{\,2} + \tilde{m}_\Lambda^2\right]^3}, \tag{14}$$

where the explicit form of $\mathcal{R}_1^\perp$ is expressed in terms of incomplete gamma functions and can be found in Appendix C of [15]. Due to its simpler Dirac-trace structure the Boer–Mulders function for a scalar diquark is much easier to calculate. The light-cone divergences encountered in the axial-vector diquark sector do not appear (see [15] for details), we find

$$h_1^{\perp,{\rm sc}}(x, \vec{p}_{\rm T}^{\,2}) = \frac{e_q e_{dq} N_{\rm sc}^4}{4(2\pi)^4} \frac{(1-x)^5 \mathrm{e}^{-\tilde{b}(\vec{p}_{\rm T}^{\,2} + 2x m_s^2 - 2x(1-x)M^2)} \mathcal{R}_1^{\perp,{\rm sc}}\left(x, \vec{p}_{\rm T}^{\,2}; R_g, \tilde{b}, \Lambda, \{\mathcal{M}\}\right)}{\vec{p}_{\rm T}^{\,2}[\vec{p}_{\rm T}^{\,2} + \tilde{m}_\Lambda^2]^3}. \tag{15}$$

In a similar manner, the Sivers function is projected from the trace of the quark–quark correlator (2) (see e.g. [14]),

$$\frac{M S_{\rm T}^i \epsilon_{\rm T}^{ij} p_{\rm T}^j}{4} f_{1{\rm T}}^\perp(x, \vec{p}_{\rm T}^{\,2}) = \int \mathrm{d}p^- \left(\mathrm{Tr}[\gamma^+ \Phi(p; P, S_{\rm T})] - \mathrm{Tr}[\gamma^+ \Phi(p; P, -S_{\rm T})]\right)\Big|_{p^+ = xP^+}.$$

While in the scalar diquark approximation, $h_1^\perp$ and $f_{1{\rm T}}^\perp$ coincide [10], the different Dirac structure for the chiral-even $f_{1{\rm T}}^\perp$ and chiral-odd $h_1^\perp$ in the axial-vector diquark sector (see eqs (11) and (16)) lead to different coefficients in the decomposition $N^{(i)}_{\alpha_1\ldots\alpha_i}$ [15]. We fix the model parameters such as masses and normalization

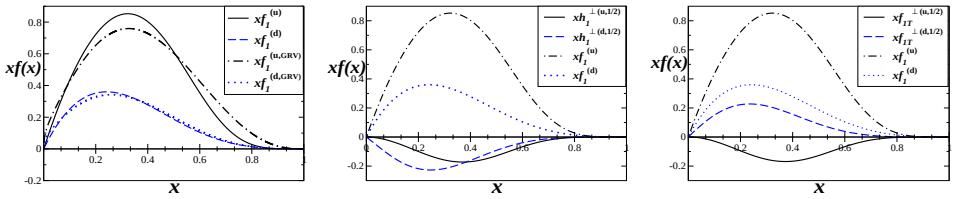


Figure 2. Left panel: The unpolarized u- and d-quark distribution functions vs. x compared to the low scale parametrization of the unpolarized u- and d-quark distributions [36]. Center panel: The half-moment of the Boer–Mulders function vs. x compared to the unpolarized u- and d-quark distribution functions. Right panel: The half moment of the Sivers functions compared to the unpolarized u- and d-quark distributions.

constants by comparing the model result for the unpolarized f_1 for u- and d-quarks to the low-scale ($\mu^2 = 0.26$ GeV) data parametrization of GRV [36]. Note that PDFs for u and d quarks are given by linear combinations of PDFs for an axial-vector and scalar diquark, $u = \frac{3}{2}f^{\rm sc} + \frac{1}{2}f^{\rm ax}$ and $d = f^{\rm ax}$ [18,30]. For 'T-odd' PDFs we fix the sign and the strength of the final-state interactions, the product of the charges of the diquark and quark, by comparing $f_{1\rm T}^{\perp}$ for u- and d-quarks in the diquark model with the existing data parametrizations (see refs [38–40]). We display the 'one-half'

$$f_{1\rm T}^{\perp(q,1/2)}(x) = \int {\rm d}^2 p_{\rm T} \frac{|\vec{p}_{\rm T}|}{M} f_{1\rm T}^{\perp(q)}(x, \vec{p}_{\rm T}^{\,2}), \tag{16}$$

moment for u- and d-quark Sivers functions $f_{1\rm T}^{\perp(q)}$ and Boer–Mulders functions $h_1^{\perp(q)}$ (where $q = u, d$) along with the unpolarized u- and d-quark pdfs in figure 2. The u- and d-quark Sivers functions are negative and positive respectively while both the u- and d-quark Boer–Mulders functions are negative over the full range in Bjorken-x. These results are in agreement with the large N_c predictions [41], Bag Model results reported in [42], impact parameter distortion picture of Burkardt [43] and recent studies of nucleon transverse spin structure in lattice QCD [44]. Also, we explored the relative dependence of the d-quark to u-quark Sivers function [15]. Choosing a value of $\kappa = -0.333$ as was determined in [35] we find that the d-quark Sivers is smaller than the u-quark. Choosing $\kappa = 1$ we find reasonable agreement with extractions reported in [38]. It is worth noting (see figure 2) that the resulting u-quark Sivers function and Boer–Mulders function are nearly equal, even with the inclusion of the axial-vector spectator diquark [10].

2.3 *Collins fragmentation function and the* $\cos(2\phi)$*-asymmetry in SIDIS*

Sometime ago it was observed that both kinematic [45] and dynamical [46] subleading twist effects could give rise to a $\cos 2\phi$ azimuthal asymmetry going like $p_{\rm T}^2/Q^2$ (where Q is a hard scale) when transverse momentum scales are on the order of the intrinsic momentum scales of partons, $P_{\rm T} \sim p_{\rm T}$. By contrast, taking into account the existence of 'T-odd' TMDs and fragmentation functions it was

pointed out by Boer and Mulders [4] that at leading twist a convolution of the Boer–Mulders and the Collins functions would give rise to non-trivial azimuthal asymmetries in unpolarized SIDIS. Thus, having studied the flavour dependence of the $h_1^\perp$ we consider the spin-independent 'T-odd' $\cos 2\phi$ contribution for π^+ and π^- production to the unpolarized cross-section

$$\frac{\mathrm{d}\sigma}{\mathrm{d}x\,\mathrm{d}y\,\mathrm{d}z\,\mathrm{d}\phi_h\,\mathrm{d}P_{h\perp}^2} = \frac{2\pi\alpha^2}{xyQ^2}\left[\left(1-y+\frac{1}{2}y^2\right)F_{UU,T}+(1-y)\cos(2\phi_h)\,F_{UU}^{\cos 2\phi_h}\right], \quad (17)$$

where the structure function $F_{UU}^{\cos 2\phi_h}$ involves a convolution of the Boer–Mulders and Collins fragmentation function

$$F_{UU}^{\cos 2\phi_h} = \mathcal{C}\left[-\frac{2\hat{\boldsymbol{h}}\cdot\boldsymbol{k}_{\mathrm{T}}\hat{\boldsymbol{h}}\cdot\boldsymbol{p}_{\mathrm{T}}-\boldsymbol{k}_{\mathrm{T}}\cdot\boldsymbol{p}_{\mathrm{T}}}{MM_h}h_1^\perp H_1^\perp\right], \quad (18)$$

where $\mathcal{C}$ represents the momentum convolution integral [4,14]. The Collins mechanism [17] describes the spin transfer of an initial state transverse polarization to the final state fragmenting quark. The Collins function is a measure of the spin asymmetry in the azimuthal distribution of the out-going hadron about the jet axis of the fragmenting quark. The probability to produce hadron h from a transversely polarized quark q, in, e.g., the $q\bar{q}$ rest frame if the fragmentation takes place in e^+e^- annihilation, is given by (see [16])

$$D_{h/q^\uparrow}(z,K_{\mathrm{T}}^2) = D_1^q(z,K_{\mathrm{T}}^2)+H_1^{\perp q}(z,K_{\mathrm{T}}^2)\frac{(\hat{\boldsymbol{k}}\times\boldsymbol{K}_{\mathrm{T}})\cdot\boldsymbol{s}_q}{zM_h}, \quad (19)$$

where M_h is the hadron mass, k is the momentum of the quark, s_q is its spin vector, z is the light-cone momentum fraction of the hadron with respect to the fragmenting quark, and K_{T} is the component of the hadron's momentum transverse to k. D_1^q is the TMD unpolarized FF, while $H_1^{\perp q}$ is the Collins function. Therefore, $H_1^{\perp q}>0$ corresponds to a preference of the hadron to move to the left if the quark is moving away from the observer and the quark spin is pointing upwards. We calculated the Collins functions in the spectator framework [16] where the fragmentation functions are calculated from the colour gauge invariant quark–quark correlation function [14]

$$\Delta(z,k_{\mathrm{T}}) = \frac{1}{2z}\sum_X\int\frac{\mathrm{d}\xi^+\mathrm{d}^2\boldsymbol{\xi}_{\mathrm{T}}}{(2\pi)^3}\mathrm{e}^{ik\cdot\xi}\langle 0|\mathcal{U}^n_{(+\infty,\xi)}\psi(\xi)|h,X\rangle\langle h,X|\bar{\psi}(0)\mathcal{U}^n_{(0,+\infty)}|0\rangle\Big|_{\xi^-=0} \quad (20)$$

with $k^-=P_h^-/z$. The unpolarized and Collins fragmentation functions [47] are projected from eq. (20) as

$$2D_1(z,k_{\mathrm{T}}^2) = \mathrm{Tr}[\Delta_0(z,k_{\mathrm{T}})\gamma^+]$$

and

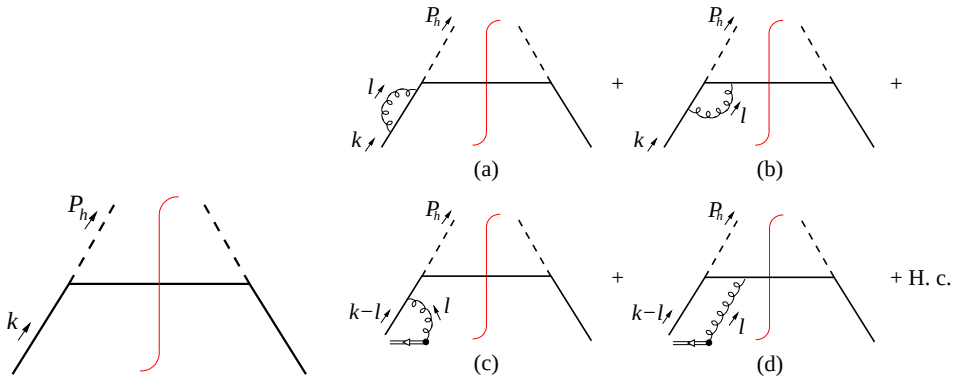


Figure 3. Left panel: Tree-level diagram for quark to meson fragmentation. Center and right panel: Single gluon-loop corrections to the fragmentation of a quark into a pion contributing to the Collins function in the eikonal approximation. 'HC' stands for the Hermitian conjugate diagrams which are not shown.

$$2\frac{\epsilon_{\mathrm{T}}^{ij}k_{\mathrm{T}j}}{M_h}H_1^{\perp}(z,k_{\mathrm{T}}^2) = \mathrm{Tr}[\Delta(z,k_{\mathrm{T}})i\sigma^{i-}\gamma_5]. \tag{21}$$

In [24,26] it was shown that the fragmentation correlators are the same in both semi-inclusive DIS and e^+e^- annihilation, as was also observed earlier in the context of a specific model calculation [24] similar to the one under consideration here. Again, we work in Feynman gauge where the transverse gauge link vanishes [6]. Employing a pseudoscalar pion–quark coupling and Gaussian form factors at the pion–quark vertex, a nonzero Collins function is generated by means of the dynamics of ISI interactions from gluons depicted in the right panel of figure 3. The Collins function is given by

$$H_1^{\perp}(z,k_{\mathrm{T}}^2) = \frac{-2\,\alpha_s g_{q\pi}^2 M_h}{(2\pi)^4}\,C_F\,\frac{\mathrm{e}^{-2k^2/\Lambda^2}}{z^2(1-z)} \times\frac{(\tilde{H}_{1(a)}^{\perp}(z,k_{\mathrm{T}}^2)+\tilde{H}_{1(b)}^{\perp}(z,k_{\mathrm{T}}^2)+\tilde{H}_{1(d)}^{\perp}(z,k_{\mathrm{T}}^2))}{k^2-m^2}, \tag{22}$$

where the subscripts in the r.h.s. refer to the contributions from figures 3a, b and d. Figure 3c gives no contribution to the Collins function. For detailed form of $\tilde{H}_{1(q)}^{\perp}$, see [16].

From the tree-level graph, left panel of figure 3 we have for the unpolarized fragmentation function D_1,

$$D_1(z,k_{\mathrm{T}}^2) = \frac{g_{q\pi}^2}{8\pi^3}\frac{\left[z^2\boldsymbol{k}_{\mathrm{T}}^2+(zm+m_s-m)^2\right]}{z^3\,(\boldsymbol{k}_{\mathrm{T}}^2+L^2)^2}, \tag{23}$$

with $L^2 = \frac{(1-z)}{z^2}M_h^2 + m^2 + \frac{m_s^2-m^2}{z}$. The parameters of the model are together with the mass of the spectator m_s and the mass of the initial quark m are fixed

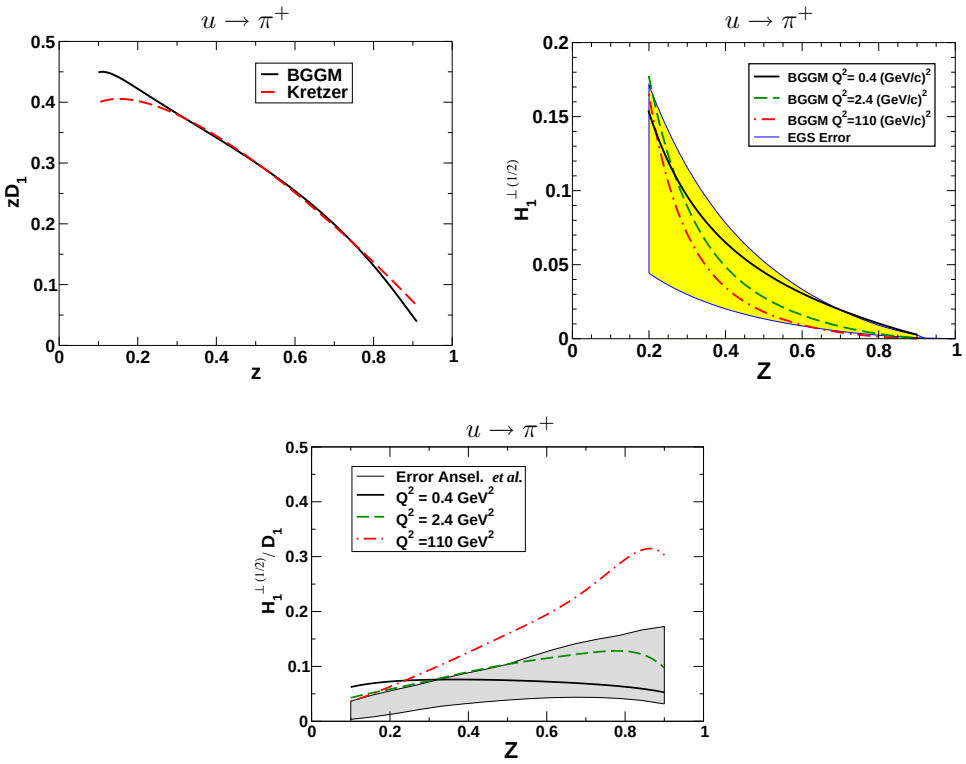


Figure 4. Left panel: Unpolarized fragmentation function $zD_1(z)$ vs. z for the fragmentation $u \to \pi^+$. Right panel: Half moment of the Collins function for $u \to \pi^+$ in our model, $H_1^{\perp(1/2)}$ at the model scale (solid line) and at a different scale under the assumption that $H_1^{\perp(1/2)}/D_1$ scales with Q^2, compared with the error band from the extraction of [49]. Bottom panel: $H_1^{\perp(1/2)}/D_1$ at the model scale (solid line) and at two other scales (dashed and dot–dashed lines) under the assumption that $H_1^{\perp(1/2)}$ does not evolve. The error band from the extraction of [50] is shown for comparison.

by performing a fit to the parametrization of [51] (NLO set) at the lowest possible scale, i.e., $Q_0 = 0.4$ GeV. The resulting values for the parameters are given in [16]. The left panel of figure 4 shows the plot of the unpolarized fragmentation function $D_1(z)$ multiplied by z for $u \to \pi^+$. The parametrization of [51] is also shown for comparison. In the right panel of figure 4, we have plotted the half moment of the Collins functions vs. z for the case $u \to \pi^+$. In the same panel, we plotted the 1-σ error band of the Collins function extracted in [49] from BELLE data, collected at a scale $Q^2 = 110$ GeV^2. In the bottom panel of figure 4, we have plotted the ratio $H_1^{\perp(1/2)}/D_1$ and compared it to the error bands of the extraction in ref. [50].

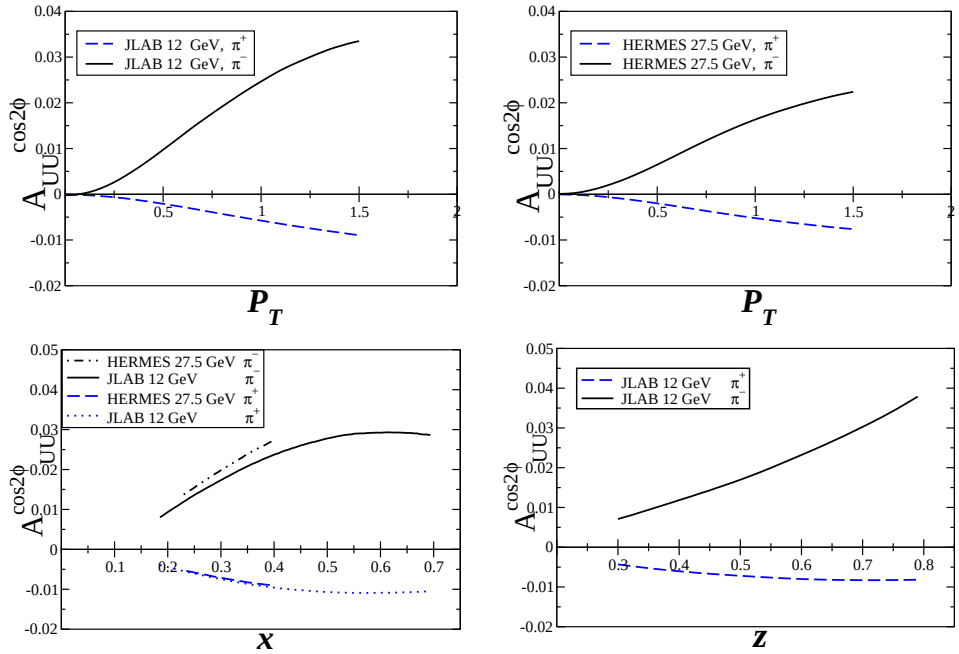


Figure 5. Upper left panel: The $\cos 2\phi$ asymmetry for π^+ and π^- as a function of $P_{\rm T}$ at JLab 12 GeV kinematics. Upper right panel: The $\cos 2\phi$ asymmetry for π^+ and π^- as a function $P_{\rm T}$ for HERMES kinematics. Bottom left panel: The $\cos 2\phi$ asymmetry for π^+ and π^- as a function of x at JLab 12 GeV and HERMES kinematics. Bottom right panel: The $\cos 2\phi$ asymmetry for π^+ and π^- as a function z for JLab kinematics.

2.4 *Azimuthal asymmetries*

Utilizing these results we calculate the double 'T-odd' contribution to the azimuthal asymmetry (eq. (18)),

$$A_{UU}^{\cos 2\phi} \equiv \frac{\int \cos 2\phi \, {\rm d}\sigma}{\int {\rm d}\sigma}. \tag{24}$$

In figure 5 we display $A_{UU}^{\cos 2\phi}(P_{\rm T})$ in the range of HERMES [2] and future JLab kinematics [52] as well as x and z dependence in the range $0.5 < P_{\rm T} < 1.5$ GeV/c. It should be noted that this asymmetry was measured at HERA by ZEUS, but at very low x and very high Q^2 [20] where other QCD effects dominate. It was also measured at CERN by EMC [53], but with low precision. Those data were approximated by Barone *et al* [54] in a u-quark dominating model for $h_1^\perp$, with a Gaussian, algebraic form and a Gaussian ansatz for the Collins function. Our dynamical approach leads to different predictions for the forthcoming JLab data.

Having calculated the chiral-odd but 'T-even' parton distribution $h_{1\rm L}^\perp$ we use this result together with the result of [16] for the Collins function to give a prediction for the $\sin(2\phi)$ single spin asymmetry A_{UL} for a longitudinally polarized target

(see also [48]). A decomposition into structure functions of the cross-section of semi-inclusive DIS for a longitudinally polarized target reads (see [14])

$$\frac{\mathrm{d}\sigma_{UL}}{\mathrm{d}x\,\mathrm{d}y\,\mathrm{d}z\,\mathrm{d}\phi_h\,\mathrm{d}P_{h\perp}^2} = \frac{2\pi\alpha^2(1-y)}{xyQ^2} S_\parallel \times \Big[\sin(2\phi_h)\, F_{UL}^{\sin(2\phi)} + \frac{(2-y)}{\sqrt{1-y}}\sin(\phi_h)\, F_{UL}^{\sin\phi}\Big], \quad (25)$$

$S_\parallel$ is the projection of the spin vector on the direction of the virtual photon. In a partonic picture the structure function $F_{UL}^{\sin(2\phi)}$ is the leading twist (while $F_{UL}^{\sin\phi}$ is sub-leading) and given by a convolution of the TMD $h_{1\mathrm{L}}^\perp$ and the Collins function [14]

$$F_{UL}^{\sin(2\phi)} = \mathcal{C}\left[-\frac{2\hat{\boldsymbol{h}}\cdot\boldsymbol{k}_\mathrm{T}\,\hat{\boldsymbol{h}}\cdot\boldsymbol{p}_\mathrm{T} - \boldsymbol{k}_\mathrm{T}\cdot\boldsymbol{p}_\mathrm{T}}{MM_h}\, h_{1\mathrm{L}}^\perp H_1^\perp\right]. \quad (26)$$

We display the results for the single spin asymmetry $A_{UL}^{\sin(2\phi)}$ in figure 6 using the kinematics of the upcoming JLab 12 GeV upgrade. We note that the π^- asymmetry is large and positive due to the model assumption $H_1^{\perp(\mathrm{dis-fav})} \approx -H_1^{\perp(\mathrm{fav})}$ [37]. This asymmetry has been measured at HERMES for longitudinally polarized protons [55] and deuterons [56]. The data show that for the proton target at HERMES 27.5 GeV kinematics both π^+ and π^- asymmetries are consistent with 0 down to a sensitivity of about 0.01. These asymmetries could be non-zero, but with magnitudes less than 0.01 or 0.02. These results are considerably smaller than our predictions for the JLab upgrade. For the deuteron target, the results are consistent with 0 for π^+ and π^-. This SIDIS data for polarized deuterons could reflect the near cancellation of u- and d-quark $h_{1\mathrm{L}}^\perp$ functions and/or the large unfavoured Collins function contributions. There is also CLAS preliminary data [57] at 5.7 GeV that shows slightly negative asymmetries for π^+ and π^- and leads to the extraction of a negative $xh_{1\mathrm{L}}^{\perp(u)}$. This suggests that the unfavoured Collins function (for $d \to \pi^+$) is not contributing much. Data from the upgrade should help resolve these phenomenological questions.

3. Summary

Here we have explored the flavour dependence leading twist 'T-odd' TMD parton distribution functions, $h_1^\perp$ (Boer–Mulders) and $f_{1\mathrm{T}}^\perp$ (Sivers) as well as the chiral odd but 'T-even' function $h_{1\mathrm{L}}^\perp$ in the diquark spectator model taking into account both axial-vector and scalar contributions. For $h_1^\perp$ we find that the k_T-half- and first-moments of this function are negative for both flavours [15] (see also [33]). Our sign result is in agreement with other approaches that predict negative $h_1^{\perp(u)}$ and $h_1^{\perp(d)}$. We also note that the resulting u-quark Sivers function and Boer–Mulders function are nearly equal, even with the inclusion of the axial-vector spectator diquark. This near equality $h_1^\perp \sim f_{1\mathrm{T}}^\perp$ was obtained from models without axial di-quarks [10], hinting at some more general mechanism that preserves the relation.

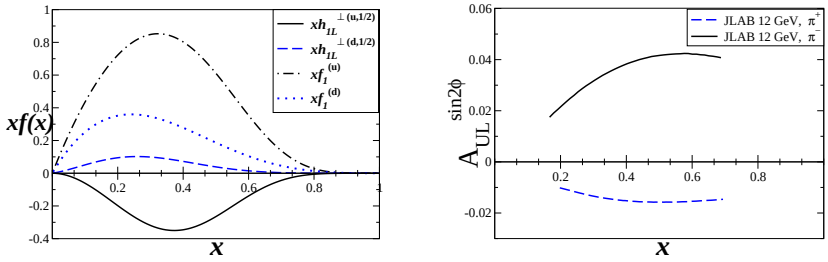


Figure 6. Left panel: The half-moment of $xh_{1L}^{\perp(1/2)}$ vs. x compared to the unpolarized u- and d-quark distribution functions. Right panel: The $\sin 2\phi$ asymmetry for π^+ and π^- as a function of x at JLAB 12 GeV kinematics.

We used our results for $h_1^\perp$ as one ingredient in the factorized formula for the azimuthal asymmetry $A_{UU}^{(\cos(2\phi))}$ in unpolarized lepto-production of positively and negatively charged pions, as well as $h_{1L}^\perp$ as an ingredient in the single-spin asymmetry $A_{UL}^{(\sin(2\phi))}$ for a longitudinally polarized target in SIDIS [15]. A key additional ingredient for determining such asymmetries is the Collins fragmentation function $H_1^\perp$. Using the most current expressions that were obtained in a similar spectator model [16], we provide estimates for $A_{UU}^{(\cos(2\phi))}$ and $A_{UL}^{(\sin(2\phi))}$. The latter has already been measured at HERMES [55] and preliminarily by CLAS [57]. There are important differences in the kinematic regions explored, but there remain discrepancies that may be resolved in the future at Jefferson Lab, for which our model gives striking predictions of relatively large asymmetries. The spirit of this work is to understand the dynamics of processes like SIDIS by refining a robust and flexible model for the 'T-odd' functions that compares with existing data.

Acknowledgements

I thank my co-authors (A Bacchetta, G R Goldstein, A Mukherjee, and M Schlegel) for fruitful collaborations which have been summarized in this contribution. This work is supported by a grant from the US Department of Energy under contract DE-FG02-07ER41460.

References

[1] D W Sivers, *Phys. Rev.* **D41**, 83 (1990)
[2] HERMES: A Airapetian *et al*, *Phys. Rev. Lett.* **94**, 012002 (2005)
[3] COMPASS: V Y Alexakhin *et al*, *Phys. Rev. Lett.* **94**, 202002 (2005)
[4] D Boer and P J Mulders, *Phys. Rev.* **D57**, 5780 (1998)
[5] J C Collins, *Phys. Lett.* **B536**, 43 (2002)
[6] A V Belitsky, X Ji and F Yuan, *Nucl. Phys.* **B656**, 165 (2003)
[7] D Boer, P J Mulders and F Pijlman, *Nucl. Phys.* **B667**, 201 (2003)
[8] S J Brodsky, D S Hwang and I Schmidt, *Phys. Lett.* **B530**, 99 (2002)
[9] X-d Ji and F Yuan, *Phys. Lett.* **B543**, 66 (2002)
[10] G R Goldstein and L Gamberg, hep-ph/0209085 (2002), *Proceedings of ICHEP 2002* (North Holland, Amsterdam, 2003) p. 452

[11] D Boer, S J Brodsky and D S Hwang, *Phys. Rev.* **D67**, 054003 (2003)
[12] L P Gamberg, G R Goldstein and K A Oganessyan, *Phys. Rev.* **D67**, 071504 (2003)
[13] P J Mulders and R D Tangerman, *Nucl. Phys.* **B461**, 197 (1996)
[14] A Bacchetta *et al*, *J. High Energy Phys.* **02**, 093 (2007)
[15] L P Gamberg, G R Goldstein and M Schlegel, *Phys. Rev.* **D77**, 094016 (2008), 0708.0324
[16] A Bacchetta, L P Gamberg, G R Goldstein and A Mukherjee, *Phys. Lett.* **B659**, 234 (2008)
[17] J C Collins, *Nucl. Phys.* **B396**, 161 (1993)
[18] R Jakob, P J Mulders and J Rodrigues, *Nucl. Phys.* **A626**, 937 (1997)
[19] ZEUS: J Breitweg *et al*, *Phys. Lett.* **B481**, 199 (2000)
[20] ZEUS: S Chekanov *et al*, *Eur. Phys. J.* **C51**, 289 (2007)
[21] NA10: S Falciano *et al*, *Z. Phys.* **C31**, 513 (1986)
[22] J S Conway *et al*, *Phys. Rev.* **D39**, 92 (1989)
[23] A M Kotzinian and P J Mulders, *Phys. Lett.* **B406**, 373 (1997)
[24] A Metz, *Phys. Lett.* **B549**, 139 (2002)
[25] L P Gamberg, G R Goldstein and K A Oganessyan, *Phys. Rev.* **D68**, 051501 (2003)
[26] J C Collins and A Metz, *Phys. Rev. Lett.* **93**, 252001 (2004)
[27] L P Gamberg, A Mukherjee and P J Mulders, *Phys. Rev.* **D77**, 114026 (2008)
[28] B Pasquini, S Cazzaniga and S Boffi, arXiv:0806.2298 [hep-ph]
[29] R Ali and P Hoodbhoy, *Phys. Rev.* **D51**, 2302 (1995)
[30] A Bacchetta, A Schaefer and J-J Yang, *Phys. Lett.* **B578**, 109 (2004)
[31] Z Lu and B Q Ma, *Phys. Rev.* **D70**, 094044 (2004)
[32] L P Gamberg, D S Hwang, A Metz and M Schlegel, *Phys. Lett.* **B639**, 508 (2006)
[33] A Bacchetta, F Conti and M Radici, 0807.0323 (2008)
[34] C J Bomhof and P J Mulders, *Nucl. Phys.* **B795**, 409 (2008)
[35] G R Goldstein and J Maharana, *Nuovo Cimento* **A59**, 393 (1980)
[36] M Gluck, E Reya and A Vogt, *Eur. Phys. J.* **C5**, 461 (1998)
[37] A Schafer and O V Teryaev, *Phys. Rev.* **D61**, 077903 (2000)
[38] M Anselmino *et al*, *Phys. Rev.* **D72**, 094007 (2005)
[39] W Vogelsang and F Yuan, *Phys. Rev.* **D72**, 054028 (2005)
[40] J C Collins *et al*, *Phys. Rev.* **D73**, 014021 (2006)
[41] P V Pobylitsa, hep-ph/0301236 (2003)
[42] F Yuan, *Phys. Lett.* **B575**, 45 (2003)
[43] M Burkardt, *Phys. Rev.* **D72**, 094020 (2005)
[44] QCDSF: M Gockeler *et al*, *Phys. Rev. Lett.* **98**, 222001 (2007)
[45] R N Cahn, *Phys. Lett.* **B78**, 269 (1978)
[46] E L Berger, *Phys. Lett.* **B89**, 241 (1980)
[47] D Amrath, A Bacchetta and A Metz, *Phys. Rev.* **D71**, 114018 (2005)
[48] A V Efremov, K Goeke and P Schweitzer, *Phys. Rev.* **D67**, 114014 (2003)
[49] A V Efremov, K Goeke and P Schweitzer, hep-ph/0603054 (2006)
[50] M Anselmino *et al*, *Phys. Rev.* **D75**, 054032 (2007)
[51] S Kretzer, *Phys. Rev.* **D62**, 054001 (2000)
[52] H Avakian *et al*, Approved JLab proposal PR 12-06-112 (2006)
[53] European Muon: M Arneodo *et al*, *Z. Phys.* **C34**, 277 (1987)
[54] V Barone, Z Lu and B-Q Ma, *Phys. Lett.* **B632**, 277 (2006)
[55] HERMES: A Airapetian *et al*, *Phys. Rev. Lett.* **84**, 4047 (2000)
[56] HERMES: A Airapetian *et al*, *Phys. Lett.* **B562**, 182 (2003)
[57] CLAS: H Avakian *et al*, *AIP Conf. Proc.* **792**, 945 (2005)